Supplementary Information

ALS/FTLD-linked mutations in FUS glycine residues cause accelerated gelation and reduced interactions with wild-type FUS

Kevin Rhine[1,2], Monika A. Makurath[3,4], James Liu[2.5], Sophie Skanchy[6], Christian Lopez[2], Kevin F. Catalan[1,2], Ye Ma[7], Taekjip Ha[1,4,6,7,8], Yann R. Chemla[4], Sua Myong[1,4,6,9]

1 Program in Cell, Molecular, Developmental Biology, and Biophysics, Johns Hopkins University, 3400 N Charles St, Baltimore, MD 21218, USA.
2 Department of Biology, Johns Hopkins University, 3400 N Charles St, Baltimore, MD 21218, USA.
3 Department of Molecular and Integrative Physiology, University of Illinois at Urbana-Champaign, Urbana, IL 61801, USA.
4 Department of Physics, Center for the Physics of Living Cells, University of Illinois at Urbana-Champaign, Urbana, IL 61801, USA.
5 Medical Genetics and Ophthalmic Genomics Unit, National Eye Institute, National Institutes of Health, Bethesda, MD 20892, USA.
6 Department of Biophysics, Johns Hopkins University, 3400 N Charles St, Baltimore, MD 21218, USA.
7 Department of Biomedical Engineering, Johns Hopkins Medical Institute, 615 N Wolfe St, Baltimore, MD 21231, USA.
8 Howard Hughes Medical Institute, Baltimore, MD, 21218, USA.
9 Lead Contact

Supplementary Information includes:

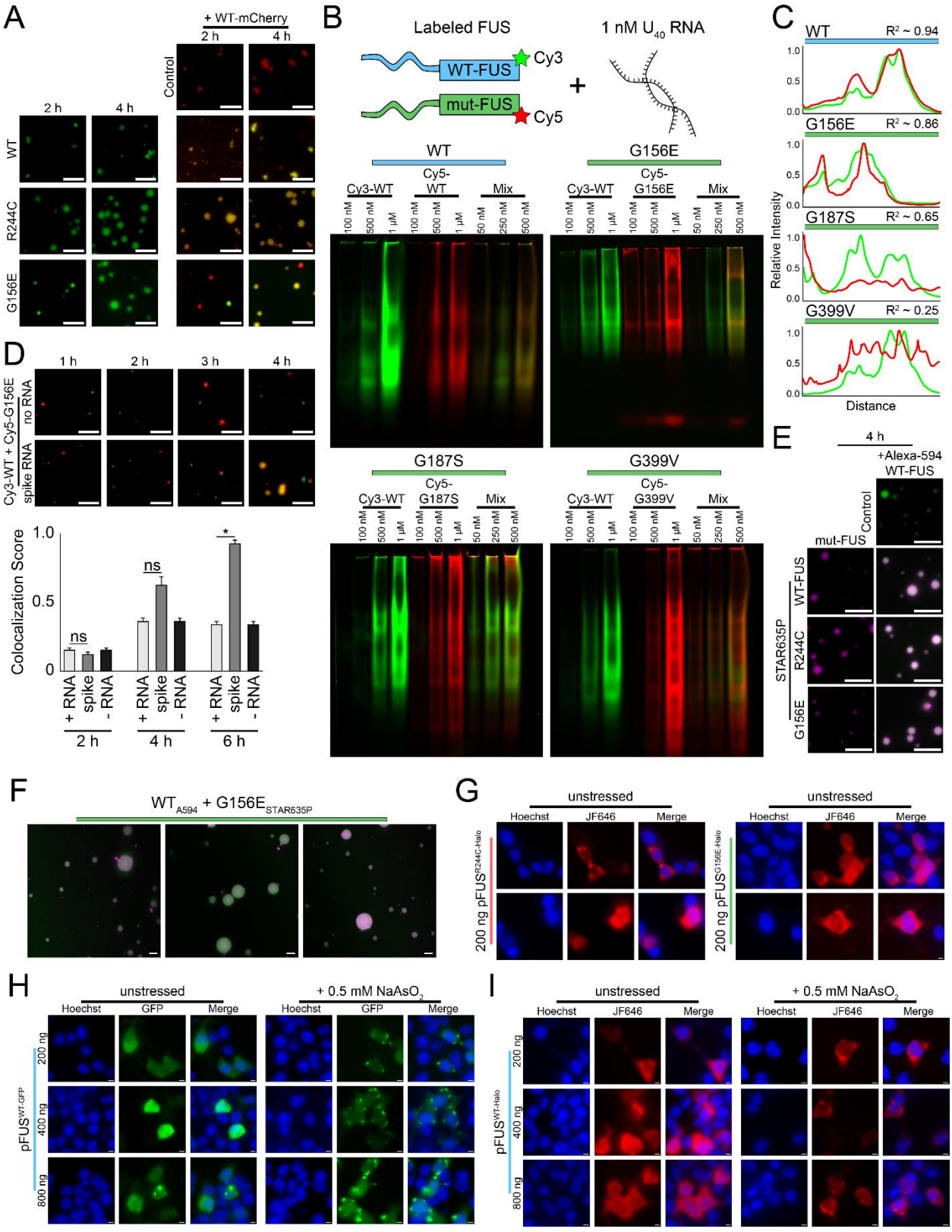

Supplemental Figure 1 (related to Figure 1): G mutant and wild-type separation occurs in gel-shift assays, condensates, and cells. (A) Wide-field images of 500 nM WT and 500 nM

mutant FUS (mixed 1:100 mCherry-/GFP-labeled:unlabeled) at 2 h and 4 h. Images were acquired in both the GFP and Cy3 (mCherry) channels and overlaid using Fiji and Adobe Photoshop CC 2019. The scale bar is 5 μm. **(B)** Cy3-WT and Cy5-mutant FUS were combined with 1 nM unlabeled pdU_{50} to undergo binding for 45 min. Samples were then electrophoresed on a 6% DNA Retardation Gel for 1.5 h at 100 V. Gels were imaged in the Cy3 and Cy5 channels on a Typhoon 5 imager at ~500 V for each channel. The acquired images were processed and overlaid in Fiji and Adobe Photoshop CC 2019. **(C)** Intensity plots of each 500 nM mixture lane were calculated using Fiji and normalized to the maximum intensity for each channel (Cy3 = green, Cy5 = red) in that lane. Pearson's correlation coefficients were calculated for the Cy3 and Cy5 channels using R Studio. **(D)** Wide-field images of 500 nM Cy3-WT and 500 nM Cy5-G156E without RNA and with RNA spiked at the 2 h timepoint. The scale bar is 5 μm. Colocalization is shown for 2 h and 4 h for + RNA (white), spiked RNA (gray) and no RNA (black), and the error bars denote SEM. Significance was determined using a two-sample proportion z-test where ns = not significant and * = $p < 0.05$. **(E)** Wide-field images of STAR635P-labeled mutant FUS and Alexa 594-labeled WT FUS at 4 h. Unlabeled FUS was mixed with labeled FUS at a 1:100 ratio. Images were acquired in the Cy3 (Alexa 594) and Cy5 (STAR635P) channels and overlaid using Fiji and Adobe Photoshop CC 2019. The scale bar is 5 μm. **(F)** Additional STED images of Alexa-594-labeled WT FUS with STAR-635P-G156E FUS after 4 h of incubation. Unlabeled FUS was 1 μM concentration whereas labeled FUS was 10 nM. The scale bar is 500 nm. **(G)** Wide-field images of $pFUS^{R244C\text{-}Halo}$ and $pFUS^{G156E\text{-}Halo}$ $pFUS^{WT\text{-}GFP}$ in the Hoechst and GFP channels. Hoechst 33342 stain was added 15 min prior to imaging. Overlays were generated with Fiji and Adobe Photoshop. The scale bar is 5 μm. **(H)** Same as (G) but with $pFUS^{WT\text{-}GFP}$ and imaged in the GFP channel instead of the Cy5 channel. Cells are shown before and after 0.5 mM $NaAsO_2$ stress for 1 h. The plasmid was added at different concentrations for transfection. **(H)** Same as (H) but with $pFUS^{WT\text{-}Halo}$ and imaged in the Cy5 channel. JF646 fluorophore (25 nM) was added 15 min prior to imaging.

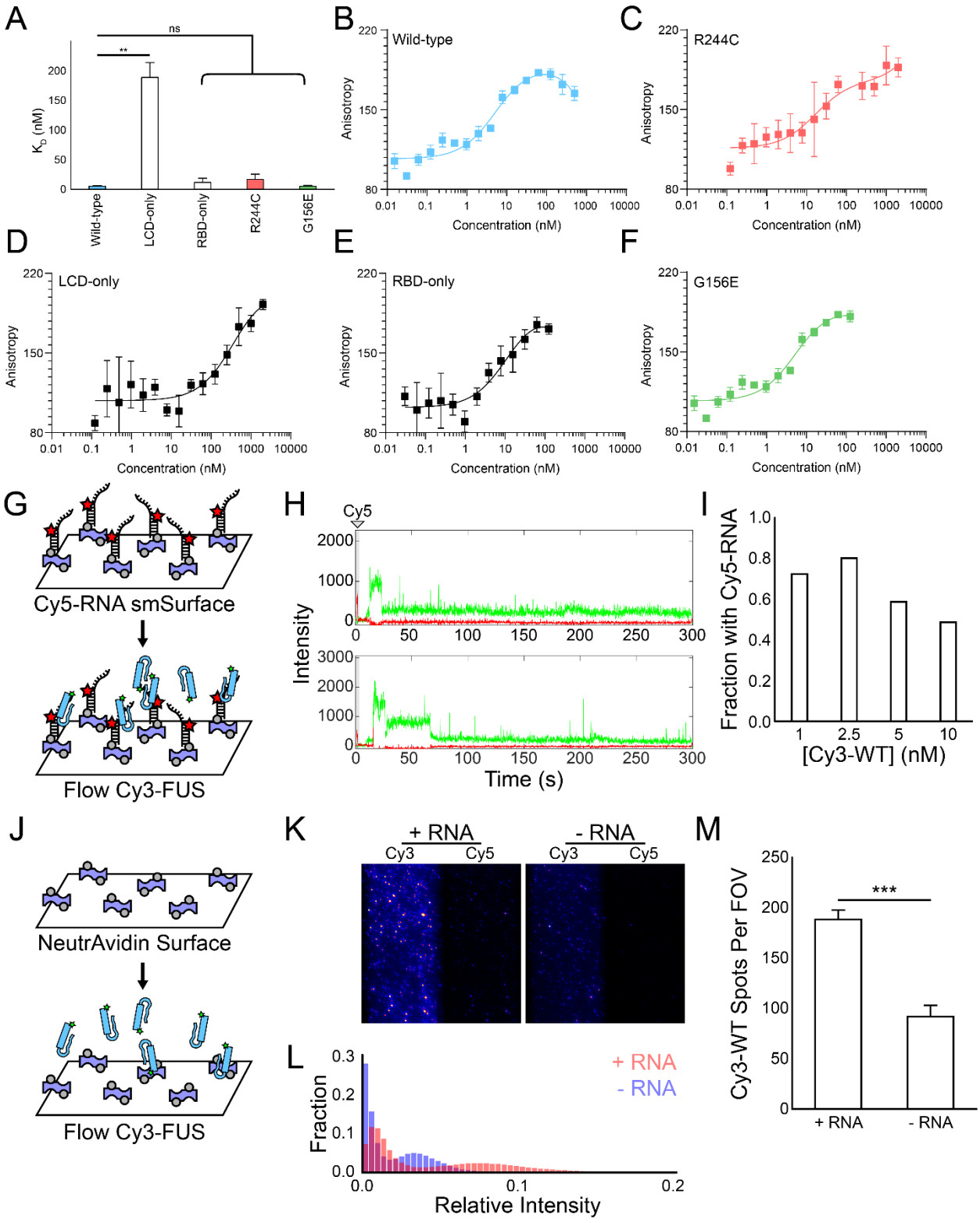

Supplemental Figure 2 (related to Figure 2): Cy-labeled FUS preferentially binds to RNA on the single-molecule surface. (A) Summary of K_D values calculated from triplicate fluorescence

anisotropy experiments. Error bars denote standard deviation, and statistics were calculated using a two-tailed two-sample Student's t-test with ns = not significant and ** = $p < 0.01$. Degrees of freedom were set at 2. **(B-F)** Fluorescence anisotropy plots for **(B)** WT, **(C)** LCD-only, **(D)** RBD-only, **(E)** R244C, and **(F)** G156E FUS. Protein was titrated from picomolar-range concentrations to micromolar-range concentrations with 10 nM Cy5-U_{40} RNA and anisotropy was measured using a Tecan plate reader. Error bars denote standard error of the mean for each data point. **(G)** Schematic showing Cy5-labeled RNA immobilized on the single-molecule surface. **(H)** Sample intensity traces (Cy3 = green, Cy5 = red) showing Cy3-WT FUS binding to traces with Cy5-RNA signal at the beginning of the trace when Cy5 excitation is used. **(I)** Quantification of the fraction of traces with Cy5-RNA signal for increasing Cy3-WT flow concentrations. **(J)** Schematic showing the single-molecule experiment with no RNA immobilized on the surface. **(K)** Still images of the single-molecule surface with and without RNA flowed in following neutravidin binding. Both the Cy3 and Cy5 channels are shown following 2.5 nM Cy3-WT flow. **(L)** Intensity histograms of the images from (K). **(M)** Quantification of the number of spots identified by the IDL mapping software for 10 images with and without RNA flow. Error is SEM. Statistics were calculated using a two-tailed two-sample Student's t-test where *** = $p < 0.001$. Degrees of freedom were set to 9.

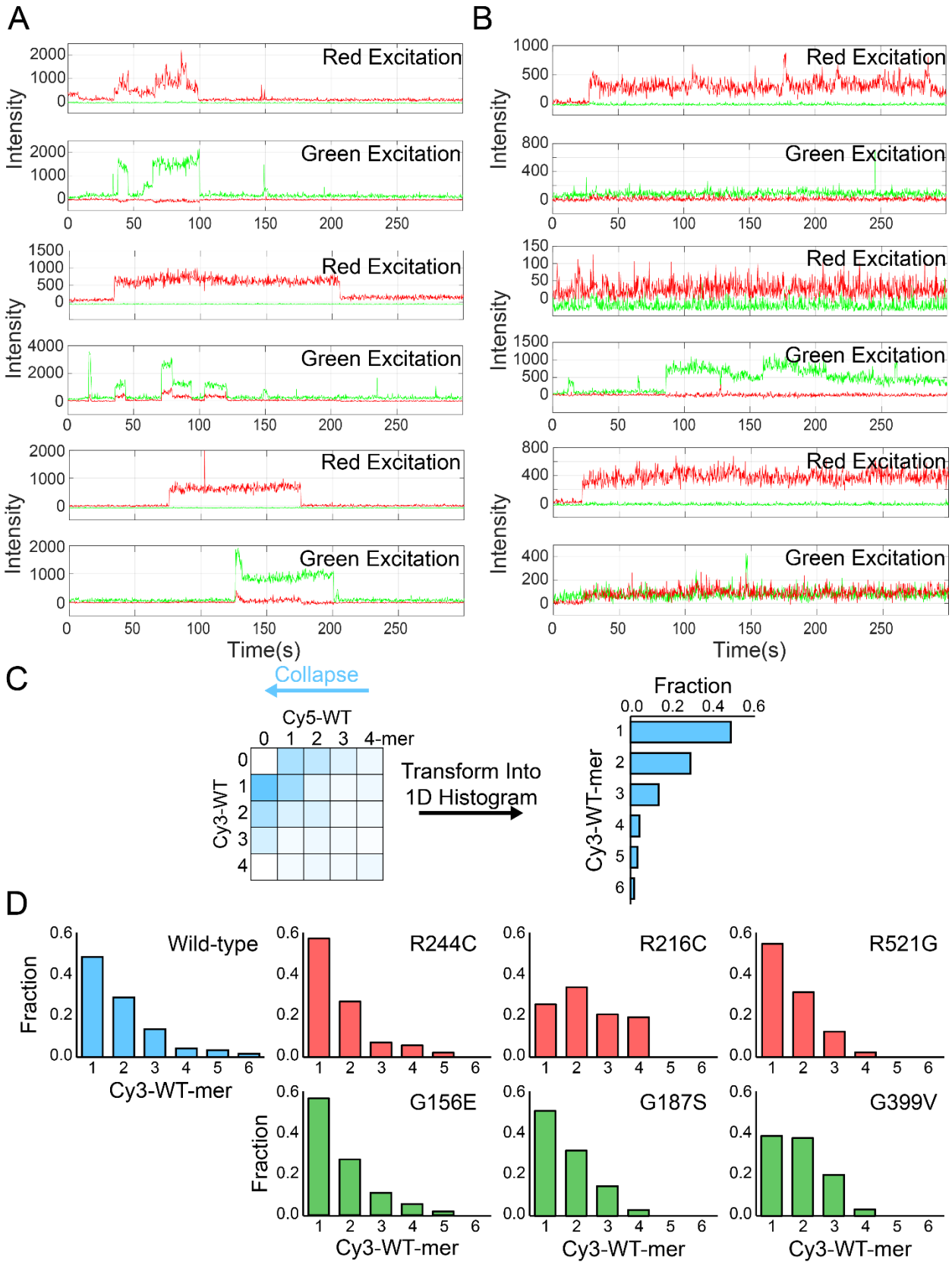
A
B
Red Excitation
Green Excitation
Intensity
Time(s)
C
Collapse
Cy5-WT
Cy3-WT
4-mer
Transform Into
1D Histogram
Fraction
Cy3-WT-mer
D
Wild-type
R244C
R216C
R521G
G156E
G187S
G399V

Supplemental Figure 3 (related to Figure 3): Addition of Cy5-mutant does not drive increased aggregation of Cy3-WT at the single-molecule level. (A) Single-molecule traces showing Cy3 (green) and Cy5 (red) intensity over time for a single RNA molecule with both green and red excitation lasers. Cy3-WT and Cy5-WT FUS (2.5 nM each) were flowed at 6 s. **(B)** Same as (A) but with 2.5 nM Cy3-WT and 2.5 nM Cy5-G156E. **(C)** Schematic detailing how Cy3-WT histograms were generated from 2D heatmaps by collapsing the y-axis. **(D)** Frequency histograms of Cy3-WT-mer status for each two-color nucleation experiment (2.5 nM Cy3-WT + 2.5 nM Cy5-mutant).

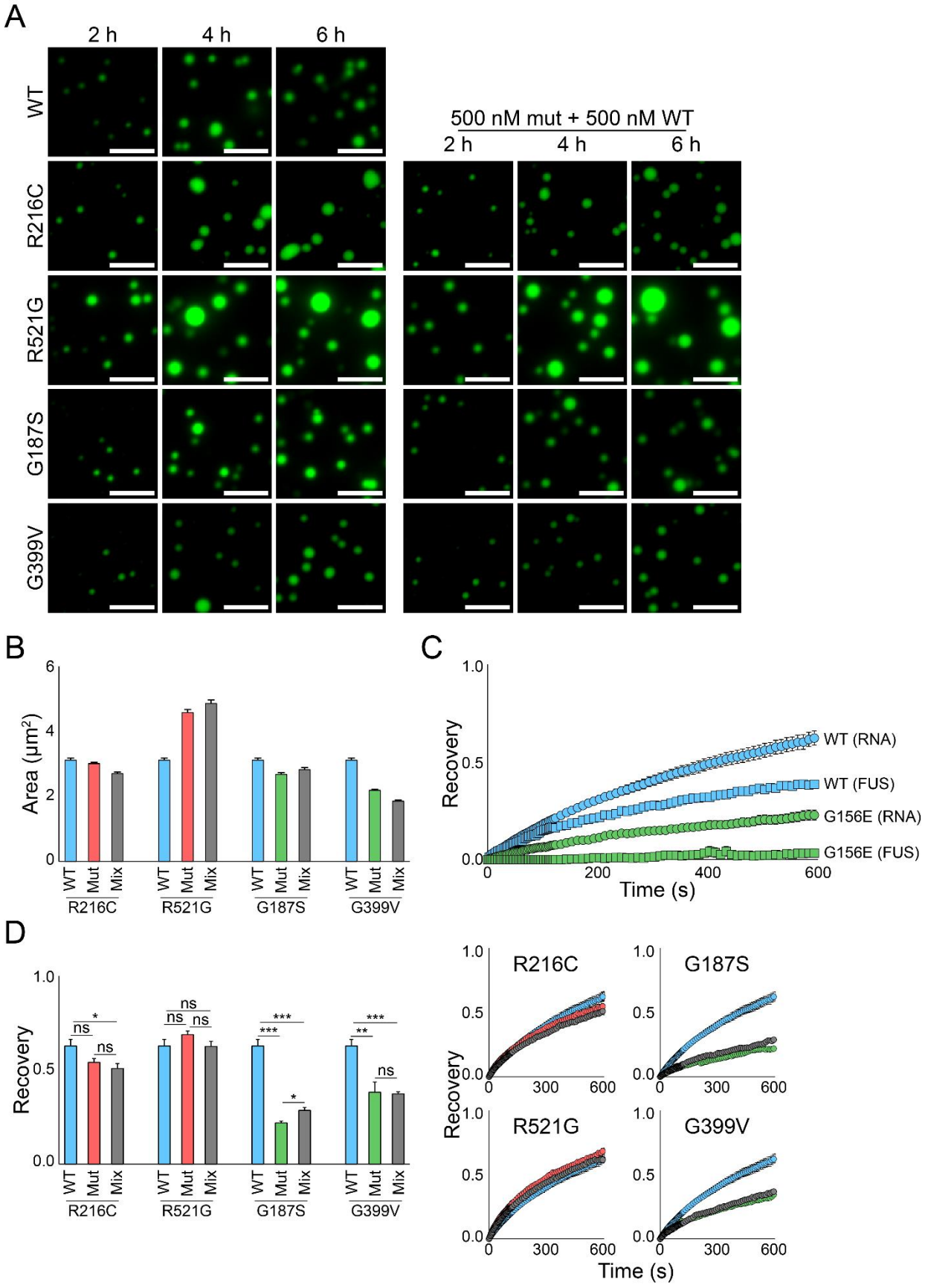
A
2 h
4 h
6 h
WT
R216C
R521G
G187S
G399V
500 nM mut + 500 nM WT
2 h
4 h
6 h
B
Area (μm²)
WT
Mut
Mix
R216C
R521G
G187S
G399V
C
Recovery
WT (RNA)
WT (FUS)
G156E (RNA)
G156E (FUS)
Time (s)
D
Recovery
ns
*
**
***
R216C
R521G
G187S
G399V
Time (s)

Supplemental Figure 4 (related to Figure 5): G187S and G399V gelation is also not recovered by addition of wild-type FUS. (A) Wide-field images of R216C, R521G, G187S, and G399V FUS with and without wild-type FUS at the 4 h time point. **(B)** Quantification of the area of FUS condensates at the 4 h timepoint. Error bars denote SEM. **(C)** FRAP curves of FUS (1 μM) with Cy3-U_{40} (1 μM) or Cy3-FUS (4 μM) with unlabeled U_{40} (250 nM): blue circles = WT RNA FRAP, blue squares = WT protein FRAP, green circles = G156E RNA FRAP, and green squares = G156E protein FRAP. Error is SEM. **(D)** FRAP quantification at 600 s (left) and curves (right) for the heterotypic and homotypic conditions in (A) at the 4 h time point. Significance was calculated using a two-sample t-test where ns = not significant, * = $p < 0.05$, ** = $p < 0.01$, and *** = $p < 0.001$.

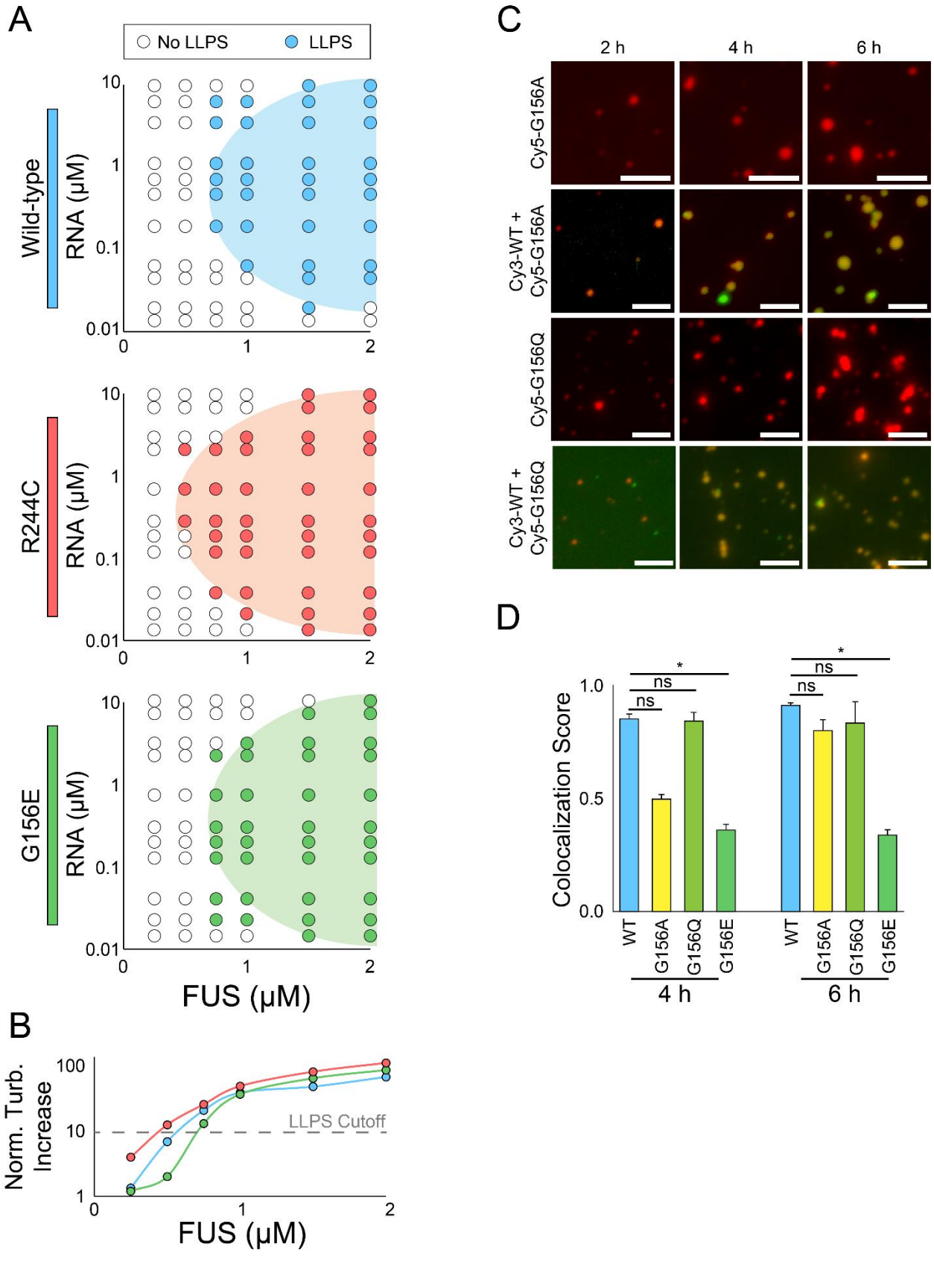
A
No LLPS
LLPS
Wild-type
R244C
G156E
RNA (μM)
10
1
0.1
0.01
0
1
2
FUS (μM)
B
Norm. Turb. Increase
100
10
1
LLPS Cutoff
FUS (μM)
C
2 h
4 h
6 h
Cy5-G156A
Cy3-WT + Cy5-G156A
Cy5-G156Q
Cy3-WT + Cy5-G156Q
D
Colocalization Score
1.0
0.5
0.0
*
ns
WT
G156A
G156Q
G156E
4 h
6 h

Supplemental Figure 5 (related to Figure 6): G156A and G156Q efficiently mix with WT FUS. **(A)** Phase diagrams of WT (blue), R244C (red), and G156E (green) FUS with U_{40} RNA. Turbidity was measured over 4 h in a 96-well plate to determine phase separation propensity (see **Methods**). LLPS-favorable conditions are indicated with filled circles, whereas unfilled circles denote conditions in which significant turbidity increases were not observed. **(B)** An example of the normalized turbidity increases for WT (blue), R244C (red), and G156E (green) FUS with 500 nM RNA at varying concentrations of FUS. The gray dashed line indicates the normalized increase corresponding with LLPS-favorable conditions. **(C)** Wide-field images of Cy5-G156A and Cy5-G156Q alone and Cy3-WT with Cy5-G156A and Cy5-G156Q at 2 h, 4 h, and 6 h. The scale bar is 5 μm. **(D)** Quantification of colocalization in (A) where error is SEM. Statistics were calculated using a two-sample proportion z-test with ns = not significant and * = $p < 0.05$.

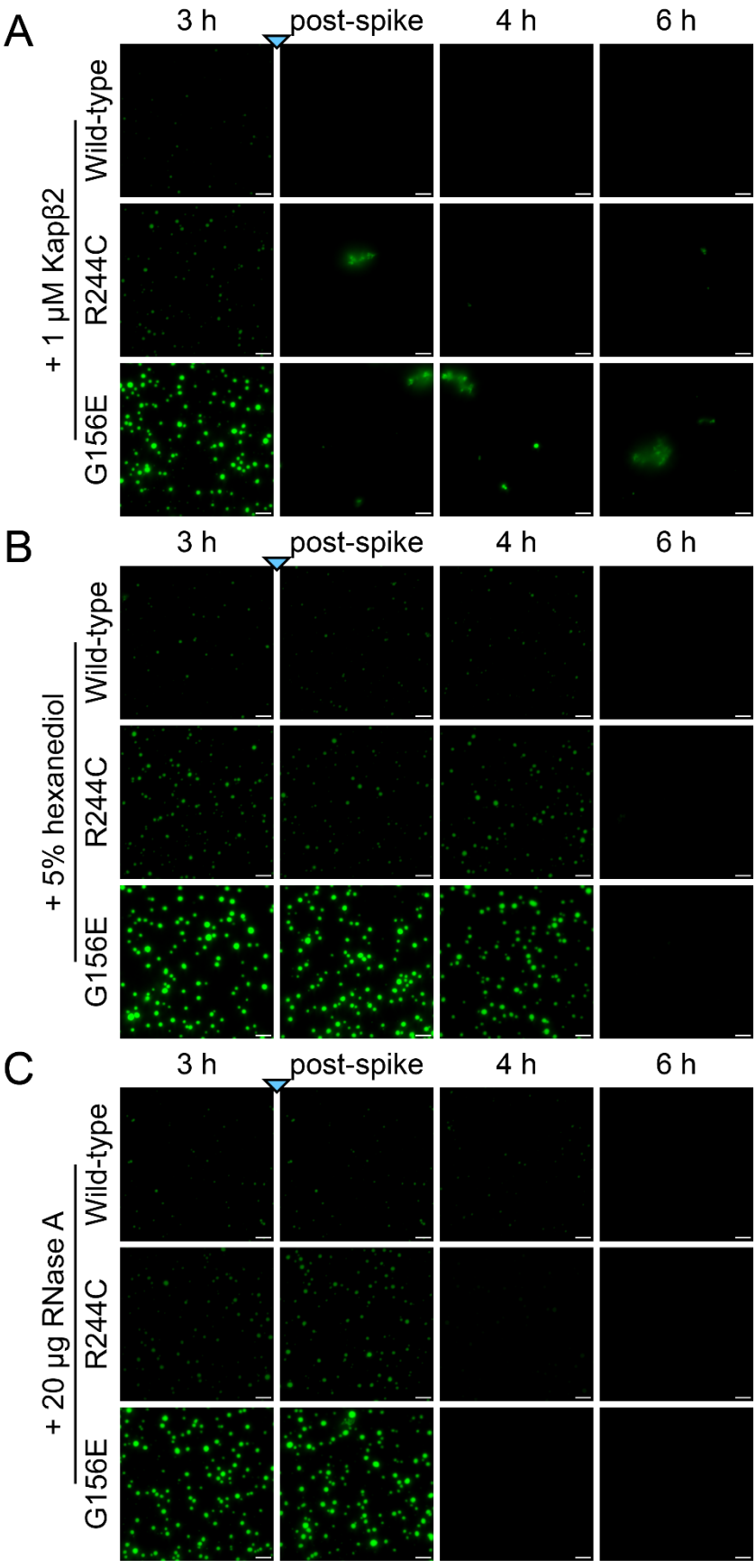
A
3 h
post-spike
4 h
6 h
+ 1 μM Kapβ2
Wild-type
R244C
G156E
B
3 h
post-spike
4 h
6 h
+ 5% hexanediol
Wild-type
R244C
G156E
C
3 h
post-spike
4 h
6 h
+ 20 μg RNase A
Wild-type
R244C
G156E

Supplemental Figure 6 (related to Figure 7): Known disaggregases dissolve WT, R244C, and G156E FUS condensates. (A) Wide-field images of 1 μM WT, R244C, and G156E FUS droplets with 1 μM U_{40} RNA and 10 nM Cy3-U_{40} RNA. Images are shown at 3 h, 4 h, and 6 h time points as well as immediately following addition of 1 μM Kapβ2 at the 3 h timepoint. **(B)** Same as (A) but with 5% 1,6-hexanediol added instead. **(C)** Same as (A) but with 20 μg RNase A.

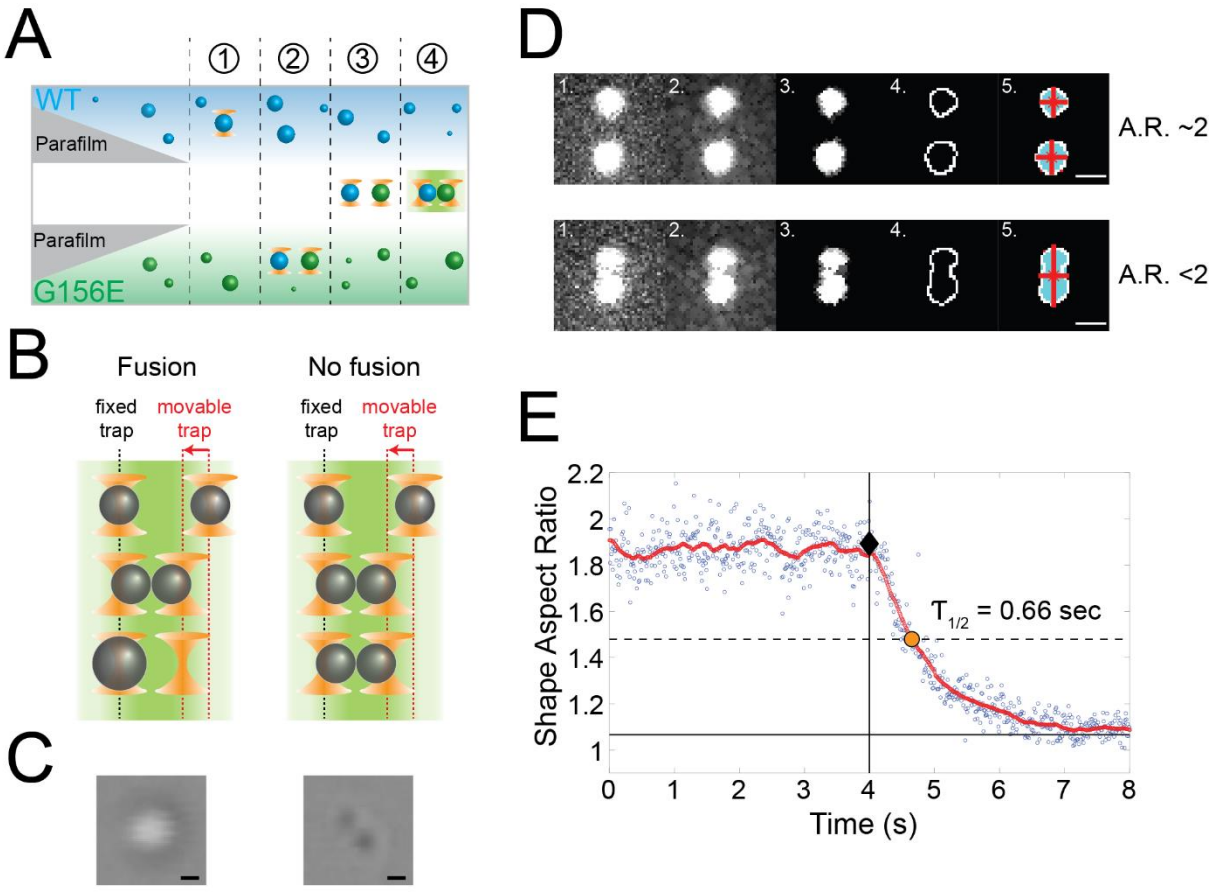

Supplemental Figure 7 (related to Figure 7 and STAR Methods): Optical trapping of fluorescent condensates. (A) Schematic of the microfluidic chamber. WT and G156E droplets are in the top and bottom laminar flow channels, respectively, which are separated by a blank channel. Droplets are trapped sequentially (steps 1-2), and are brought to the middle channel (3), where Cy3-labelled RNA is excited by a green excitation laser (4). **(B)** During a fluorescence measurement, the droplet pair is brought into close proximity by decreasing the separation between the optical traps. A fused droplet falls into one of the traps, while unfused droplets remain in separate traps. **(C)** Brightfield image of fused (left panel) and unfused (right panel) droplets released from the traps. Scale bar is 1 μm. **(D)** Steps involved in fluorescence image processing to measure the aspect ratio as described in Methods (M.8.5.). Scale bar is 1 μm. **(E)** Aspect ratio trace with the raw (100 Hz) and averaged data (50 Hz) (blue points and red line), changepoint indicating a start of fusion (black diamond and black vertical line), the end of fusion (black horizontal line), and characteristic fusion time at half-point, $\tau_{1/2}$.